

Layer and Tunnel Structures in New Molybdenophosphates: $\text{Cs}_2\text{Mo}_4\text{P}_6\text{O}_{26}$ and $M_4\text{Mo}_8\text{P}_{12}\text{O}_{52}$ ($M = \text{Cs, Rb, K, Tl}$)

K.-H. LII AND R. C. HAUSHALTER

Exxon Research and Engineering Company, Annandale, New Jersey 08801

Received October 6, 1986; in revised form December 8, 1986

Crystals of $\text{Cs}_2\text{Mo}_4\text{P}_6\text{O}_{26}$ and $\text{Cs}_4\text{Mo}_8\text{P}_{12}\text{O}_{52}$ were both discovered in the same reaction product obtained from heating a stoichiometric mixture of Cs_2MoO_4 , MoO_3 , MoO_2 , and P_2O_5 in an evacuated quartz tube at 800°C . For $\text{Cs}_2\text{Mo}_4\text{P}_6\text{O}_{26}$, monoclinic, $P2/c$, $a = 7.479(3)$, $b = 8.461(5)$, $c = 9.018(2)$ Å, $\beta = 101.99(3)^\circ$, $V = 558.2(7)$ Å³, $Z = 1$, and $R = 0.045$, $R_w = 0.053$ for 936 independent reflections. For $\text{Cs}_4\text{Mo}_8\text{P}_{12}\text{O}_{52}$, monoclinic, $P2_1$, $a = 6.398(1)$, $b = 19.497(6)$, $c = 9.835(2)$ Å, $\beta = 107.06(3)^\circ$, $V = 1173(1)$ Å³, $Z = 1$, and $R = 0.046$, $R_w = 0.058$ for 1398 independent reflections. $\text{Cs}_2\text{Mo}_4\text{P}_6\text{O}_{26}$ consists of layers of molybdenum phosphorus oxide with the cesium atoms between the layers. Each layer is built up from corner-sharing MoO_6 octahedra, PO_4 tetrahedra, and pyrophosphate groups, P_2O_7 . $\text{Cs}_4\text{Mo}_8\text{P}_{12}\text{O}_{52}$ is composed of the same building units arranged in a different way to give rise to tunnels where the cesium cations reside. The rubidium, potassium, and thallium analogs of $\text{Cs}_4\text{Mo}_8\text{P}_{12}\text{O}_{52}$ were also prepared. The $\text{Cs}_2\text{Mo}_4\text{P}_6\text{O}_{26}$ structure is closely related to that of $\text{K}_4\text{Mo}_8\text{P}_{12}\text{O}_{52}$ (A. Leclaire, J. C. Monier, and B. Raveau, *J. Solid State Chem.* **48**, 147 (1983)). © 1987 Academic Press, Inc.

Introduction

Recently, two interesting molybdenum phosphorus oxides $\text{K}_4\text{Mo}_8\text{P}_{12}\text{O}_{52}$ (1) and $\text{TlMo}_2\text{P}_3\text{O}_{12}$ (2) were reported by Leclaire and co-workers. The common features of these materials are the reduced oxidation state for molybdenum and the existence of large tunnels where the monovalent counter cations reside. In both materials the counter cations show large thermal parameters suggesting the possibility of introducing either larger metal cations or small organic ions into the tunnel without drastically modifying the framework. In an attempt to prepare a cesium analog of $\text{K}_4\text{Mo}_8\text{P}_{12}\text{O}_{52}$, two new phases with the same chemical composition, but with distinct crystal structures, were discovered in the same product. In this paper we present the

preparation and crystal structures of $\text{Cs}_2\text{Mo}_4\text{P}_6\text{O}_{26}$ and $M_4\text{Mo}_8\text{P}_{12}\text{O}_{52}$ ($M = \text{Cs, Rb, K, Tl}$). The former compound consists of layers of molybdenum phosphorus oxide with the cesium atoms between the layers. The other compounds, which are composed of the same building units as those in $\text{Cs}_2\text{Mo}_4\text{P}_6\text{O}_{26}$, have a tunnel structure with the monovalent cations in the tunnels. Because two different forms of $\text{K}_4\text{Mo}_8\text{P}_{12}\text{O}_{52}$ have been observed, those which were discovered by Leclaire *et al.* and us are referred to as the α - and β -forms, respectively.

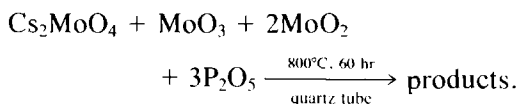
Experimental and Results

Preparation and Characterization

All manipulations were performed under He atmosphere although the reaction prod-

ucts appeared to be air-stable. MoO₂ (99.9%), MoO₃ (99.9%), K₂MoO₄ (99.9%), Rb₂MoO₄ (99.9%), Mo metal (99.9%), Tl metal (99.995%), and P₂O₅ (99.9%) were obtained from Cerac. Cs₂MoO₄ (Research Organic/Inorganic Chemical Corp., optical grade) was dried at 200°C under dynamic vacuum overnight before being used. X-ray powder diffraction patterns were obtained using a Philips powder diffractometer and filtered copper radiation. The samples were contained in a specially designed vacuum-tight cell which was fitted with a Be window. Precision peak positions were obtained using a slow scan (0.25°/min) with Si as an internal standard. The cell parameters were refined by a least-squares procedure.

The following reaction was conducted in an attempt to prepare a cesium analog of K₄Mo₈P₁₂O₅₂:



The X-ray powder pattern of the bulk product could not be indexed on the basis of the K₄Mo₈P₁₂O₅₂ structure. There were three phases in the product: the major phase occurred as brownish green plates (Cs₂Mo₄P₆O₂₆) and the minor phases as brownish green needles (Cs₄Mo₈P₁₂O₅₂) and an emerald green crystalline material. The emerald green material was present only in small amounts and has not yet been characterized. Subsequently, a few more reactions to prepare pure Cs₂Mo₄P₆O₂₆ were conducted. It was found that the product always contained the minor phases. Single-crystal X-ray structures for Cs₂Mo₄P₆O₂₆ and Cs₄Mo₈P₁₂O₅₂ have been determined (*vide infra*).

The green compounds M₄Mo₈P₁₂O₅₂ (M = Rb, K, Tl), which are isostructural with Cs₄Mo₈P₁₂O₅₂ based on their X-ray powder diffraction patterns, have been prepared by heating stoichiometric mixtures of Rb₂Mo

O₄ (K₂MoO₄ or Tl metal), MoO₂ (or Mo metal), MoO₃, and P₂O₅ in evacuated quartz tubes at 800°C. A sample of Rb₄Mo₈P₁₂O₅₂, which was single phase by X-ray analysis, was sent for elemental analysis. The results (Schwarzkopf Microanalytical Lab) were consistent with the formula and indicated that no Si was present. Anal. Calcd for Rb₄Mo₈P₁₂O₅₂: Rb, 14.78%; Mo, 33.18%; P, 16.07%. Found: Rb, 15.04%; Mo, 33.45%; P, 16.16%. The unit cell parameters for Rb₄Mo₈P₁₂O₅₂ determined from 20 accurately centered reflections using a CAD-4 four-circle diffractometer were $a = 6.3792(9)$, $b = 19.095(2)$, $c = 9.738(2)$ Å, $\beta = 107.06(1)^\circ$, $V = 1133.9(3)$ Å³. The cell parameters for β -K₄Mo₈P₁₂O₅₂ and Tl₄Mo₈P₁₂O₅₂, obtained from least-squares fit of the peak positions in the X-ray powder patterns, were $a = 6.384(5)$, $b = 18.849(7)$, $c = 9.675(4)$ Å, $\beta = 106.89(5)^\circ$, $V = 1114(1)$ Å³ and $a = 6.378(3)$, $b = 19.070(6)$, $c = 9.745(3)$ Å, $\beta = 107.02(4)^\circ$, $V = 1133.3(8)$ Å³, respectively.

Single-Crystal X-Ray Structure Determinations for Cs₂Mo₄P₆O₂₆ and Cs₄Mo₈P₁₂O₅₂

Each crystal was mounted in a glass capillary in a random orientation. All measurements were made on an Enraf-Nonius CAD-4 diffractometer using monochromatic MoK_α radiation. The cell parameters were obtained at 23°C from 25 carefully centered reflections between $7^\circ < 2\theta < 13^\circ$. Based on the systematic extinctions and the successful solution and refinement of the structures, the space groups were determined to be *P2/c* (#13) for Cs₂Mo₄P₆O₂₆ and *P2₁* (#4) for Cs₄Mo₈P₁₂O₅₂, respectively.

The intensity data were corrected for absorption, Lorentz, and polarization effects. The structures were solved by direct methods. Neutral atom scattering factors were taken from Cromer and Waber (3). Anomalous dispersion effects were

included in F_c (4); the values for $\Delta f'$ and $\Delta f''$ were those of Cromer (5). In $\text{Cs}_2\text{Mo}_4\text{P}_6\text{O}_{26}$ all of the atoms were refined anisotropically. However, in $\text{Cs}_4\text{Mo}_8\text{P}_{12}\text{O}_{52}$ the Cs and Mo atoms were refined anisotropically and all other atoms were refined isotropically, due to the limited amount of data. The occupancy factors of the Cs atoms were initially refined but the resul-

tant values were very close to 1.0. In the final cycle of refinement for each compound the Cs site was considered to be fully occupied. The last cycle of full-matrix least-squares refinement converged at $R = 0.045$ and $R_w = 0.053$ for $\text{Cs}_2\text{Mo}_4\text{P}_6\text{O}_{26}$ and $R = 0.046$ and $R_w = 0.058$ for $\text{Cs}_4\text{Mo}_8\text{P}_{12}\text{O}_{52}$. The experimental details for both compounds are listed in Table I. Posi-

TABLE I
SUMMARY OF CRYSTAL DATA, INTENSITY MEASUREMENTS, AND STRUCTURE
REFINEMENT PARAMETERS FOR $\text{Cs}_2\text{Mo}_4\text{P}_6\text{O}_{26}$ AND $\text{Cs}_4\text{Mo}_8\text{P}_{12}\text{O}_{52}$

	$\text{Cs}_2\text{Mo}_4\text{P}_6\text{O}_{26}$	$\text{Cs}_4\text{Mo}_8\text{P}_{12}\text{O}_{52}$
1. Crystal data		
Space group	$P2/c$ (#13)	$P2_1$ (#4)
Cell dimensions (296 K)	$a = 7.479(3) \text{ \AA}$ $b = 8.461(5) \text{ \AA}$ $c = 9.018(2) \text{ \AA}$ $\beta = 101.99(3)^\circ$ $V = 558.2(7) \text{ \AA}^3$	$a = 6.398(1) \text{ \AA}$ $b = 19.497(6) \text{ \AA}$ $c = 9.835(2) \text{ \AA}$ $\beta = 107.06(3)^\circ$ $V = 1173(1) \text{ \AA}^3$
Z	1	1
Density (calcd) (g/cm ³)	3.71	3.54
Crystal size (mm)	0.20 × 0.20 × 0.05	0.15 × 0.08 × 0.05
Abs. coeff. (MoK_α) (cm ⁻¹)	59.64	56.77
2. Intensity measurements		
Radiation	MoK_α	MoK_α
λ (graphite-monochromated)	0.71073 \AA	0.71073 \AA
Scan mode	$\omega/2\theta$	$\omega/2\theta$
Scan rate (in omega)	4°/min	4°/min
Scan width (degree)	0.65 + 0.35 tan θ	0.65 + 0.35 tan θ
Maximum 2θ	55°	46°
Standard refl.	3 measured every 41 min (no decay)	3 measured every 41 min (no decay)
No. of refl. measured	1411 total 1273 unique	1730 total 1679 unique
3. Structure solution and refinement		
Refl. included	936 with $F_o^2 > 3.0\sigma(F_o^2)$	1398 with $F_o^2 > 2.5\sigma(F_o^2)$
Parameters refined	89	183
Agreement factors ^a	$R = 0.045$, $R_w = 0.053$	$R = 0.046$, $R_w = 0.058$
E.s.d. of obs. of unit weight ^b	1.50	1.14
Secondary extinction coeff.	0.7032×10^{-6}	0.5418×10^{-7}
Max. peak in final diff. map	1.69 $e/\text{\AA}^3$	2.05 $e/\text{\AA}^3$

^a $R = \sum (|F_o| - |F_c|) / \sum |F_o|$; $R_w = \text{SQRT} (\sum w(|F_o| - |F_c|)^2 / \sum w F_o^2)$ with $w = 4F_o^2 / \sigma^2(F_o^2)$.

^b E.s.d. of obs. of unit weight = $\text{SQRT} [\sum w(|F_o| - |F_c|)^2 / (N_o - N_v)]$, where N_o = number of observations and N_v = number of variables.

TABLE II
POSITIONAL PARAMETERS AND B_{eq} FOR $\text{Cs}_2\text{Mo}_4\text{P}_6\text{O}_{26}$

Atom	<i>x</i>	<i>y</i>	<i>z</i>	B_{eq}^a
Cs1	1/2	0.2414(2)	3/4	5.04(7)
Mo1	0.7813(1)	0.23356(7)	0.42812(8)	0.67(3)
P1	0.0000	-0.0441(3)	1/4	0.8(1)
P2	0.8453(3)	0.5606(2)	0.6346(3)	0.80(7)
O1	0.5711(9)	0.1602(7)	0.4141(8)	1.6(2)
O2	0.879(1)	0.0555(8)	0.3286(8)	1.9(3)
O3	0.7296(8)	0.3596(7)	0.2312(7)	1.2(2)
O4	0.0589(9)	0.3269(7)	0.4499(7)	1.3(2)
O5	0.8748(8)	0.1502(7)	0.6351(7)	1.3(2)
O6	0.7304(8)	0.4382(7)	0.5350(7)	1.2(2)
O7	0.0000	0.466(1)	3/4	1.0(3)

^a The isotropic equivalent thermal parameter is defined as $B_{\text{eq}} = \frac{1}{3}[a^2\beta_{11} + b^2\beta_{22} + c^2\beta_{33} + 2ab(\cos \gamma)\beta_{12} + 2ac(\cos \beta)\beta_{13} + 2bc(\cos \alpha)\beta_{23}]$.

tional parameters and temperature factors are tabulated in Tables II and III. Selected bond distances are given in Tables IV and V. Tables of observed and calculated structure factor amplitudes, anisotropic thermal parameters, and listings of bond angles are available on request from the authors.

Description and Discussion of the Structures

$\text{Cs}_2\text{Mo}_4\text{P}_6\text{O}_{26}$

As shown in Fig. 1, the most prominent structural feature of $\text{Cs}_2\text{Mo}_4\text{P}_6\text{O}_{26}$ is the layers of molybdenum phosphorus oxide with the cesium atoms between the layers. Each layer is built up from corner-sharing octahedra and tetrahedra. Along the *b* axis the layers are composed of strips of PO_4 tetrahedra, MoO_6 octahedra, and pyrophosphate groups P_2O_7 which alternate in the following sequence: $(\text{PO}_4)(\text{MoO}_6)(\text{P}_2\text{O}_7)(\text{MoO}_6)(\text{PO}_4)$. . . The view of the layer along the *a* axis (Fig. 2) shows how the polyhedra are connected. Each of the four MoO_6 octahedra in a unit cell shares five corners with PO_4 tetrahedra or P_2O_7 groups

with the sixth corner being unshared. The molybdenum atom is coordinated to six oxygen atoms, forming a slightly distorted octahedra ($d(0-0) = 2.694$ to 2.884 Å). However, the molybdenum atom is not

TABLE III
POSITIONAL PARAMETERS AND ISOTROPIC THERMAL PARAMETERS (B) FOR $\text{Cs}_4\text{Mo}_8\text{P}_{12}\text{O}_{52}$

Atom	<i>x</i>	<i>y</i>	<i>z</i>	B^a
Cs1	0.7337(5)	0.9130	0.0039(3)	2.97(9)
Cs2	0.7146(3)	0.7472(2)	-0.3650(2)	2.14(8)
Mo1	0.4376(4)	0.0347(2)	-0.3906(3)	0.4(1)
Mo2	0.3539(4)	0.7449(2)	-0.0713(2)	0.28(9)
Mo3	0.0610(4)	0.7889(2)	0.3710(3)	0.3(1)
Mo4	0.1445(4)	0.0726(2)	0.0556(3)	0.3(1)
P1	0.236(1)	0.8766(4)	-0.3091(8)	0.3(1)
P2	0.899(1)	0.7318(4)	0.0313(7)	0.2(1)
P3	0.510(1)	0.8223(4)	0.2794(8)	0.5(1)
P4	0.257(1)	0.9457(4)	0.2931(8)	0.6(1)
P5	0.598(1)	0.0880(4)	-0.0431(8)	0.4(1)
P6	0.983(1)	0.0004(4)	-0.3000(7)	0.3(1)
O1	0.331(3)	0.998(1)	-0.591(2)	0.8(4)
O2	0.434(3)	0.117(1)	-0.442(2)	1.1(4)
O3	0.747(3)	0.009(1)	-0.384(2)	0.8(4)
O4	0.544(3)	0.052(1)	-0.186(2)	1.2(4)
O5	0.402(3)	0.925(1)	-0.329(2)	0.6(4)
O6	0.163(3)	0.822(1)	-0.422(2)	1.0(4)
O7	0.026(3)	0.918(1)	-0.308(2)	0.8(4)
O8	0.313(3)	0.841(1)	-0.165(2)	1.0(4)
O9	0.419(3)	0.668(1)	0.064(2)	0.0(3)
O10	0.288(3)	0.700(1)	-0.224(2)	0.7(4)
O11	0.681(3)	0.753(1)	-0.060(2)	0.5(3)
O12	0.455(3)	0.805(1)	0.125(2)	1.6(5)
O13	0.049(3)	0.751(1)	-0.058(2)	0.9(4)
O14	0.955(3)	0.778(1)	0.161(2)	0.6(4)
O15	0.382(3)	0.788(1)	0.363(2)	0.7(4)
O16	0.754(3)	0.815(1)	0.359(2)	0.3(3)
O17	0.479(3)	0.903(1)	0.291(2)	0.4(3)
O18	0.054(3)	0.710(1)	0.422(2)	0.8(4)
O19	0.091(3)	0.894(1)	0.313(2)	0.3(2)
O20	0.175(3)	0.979(1)	0.147(2)	0.4(4)
O21	0.084(3)	0.159(1)	-0.074(2)	0.6(4)
O22	0.220(4)	0.117(1)	0.205(2)	1.8(5)
O23	0.830(3)	0.066(1)	0.050(2)	0.4(3)
O24	0.038(3)	0.016(1)	-0.143(2)	0.4(4)
O25	0.440(3)	0.062(1)	0.038(2)	0.8(4)
O26	0.128(3)	0.034(1)	-0.379(2)	0.6(4)

^a The thermal parameters for all of the cesium and molybdenum atoms are given in isotropic equivalent thermal parameters (B_{eq}).

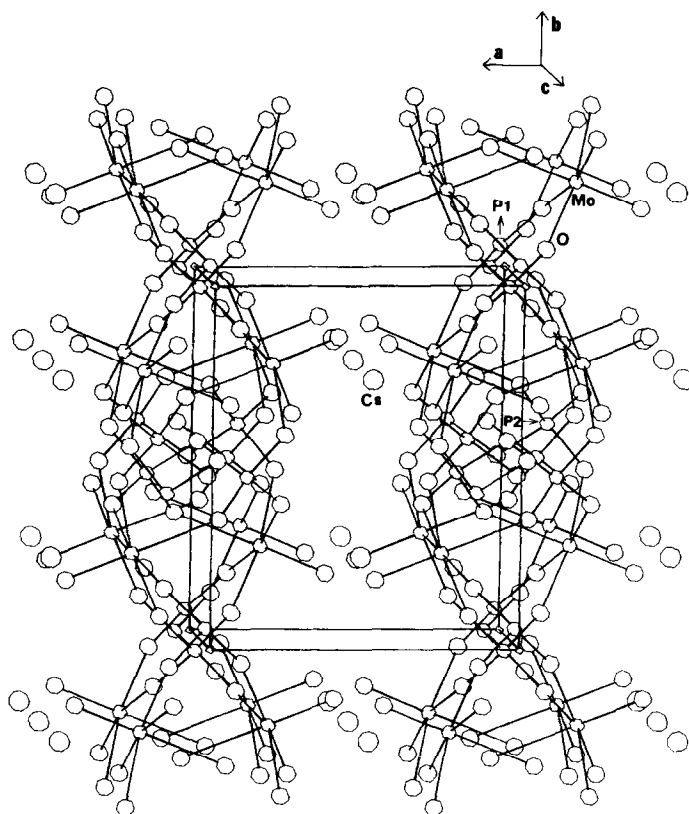


FIG. 1. A perspective view of the $\text{Cs}_2\text{Mo}_4\text{P}_6\text{O}_{12}$ structure.

centered in the octahedron, which results in one very short (1.670 Å) and one very long (2.192 Å) Mo–O bond distance (Fig. 3). As discussed by Leclaire *et al.* (1), the very

TABLE IV
SELECTED INTERATOMIC DISTANCES (Å) IN
 $\text{Cs}_2\text{Mo}_4\text{P}_6\text{O}_{26}$

Atom	Atom	Distance	Atom	Atom	Distance
Cs	O1	3.256(7) (2×)	P1	O2	1.516(7) (2×)
Cs	O5	3.276(7) (2×)	P1	O5	1.534(6) (2×)
Cs	O6	3.300(7) (2×)	P2	O3	1.509(6)
Mo	O1	1.670(6)	P2	O4	1.492(6)
Mo	O2	1.970(6)	P2	O6	1.516(6)
Mo	O3	2.038(6)	P2	O7	1.602(4)
Mo	O4	2.192(6)			
Mo	O5	1.982(6)			
Mo	O6	2.056(6)			

short Mo–O1 distance suggests a pi bonding interaction, i.e., some double bond character, between O1 and the Mo. In the compound $\alpha\text{-K}_4\text{Mo}_8\text{P}_{12}\text{O}_{52}$, a more pronounced difference between the shortest (1.66 Å) and the longest (2.28 Å) distances was observed. The oxidation state of molybdenum in $\text{Cs}_2\text{Mo}_4\text{P}_6\text{O}_{26}$ can be estimated by summing the bond strengths of Mo–O bonds. Bond strengths were calculated according to (6)

$$s = (d/1.882 \text{ \AA})^{-6.0},$$

where s = bond strength of a particular Mo–O bond, d = observed bond length, 1.881 Å = bond length of a Mo–O bond of unit valence, and -6.0 is a fitted constant. The oxidation state for Mo calculated by

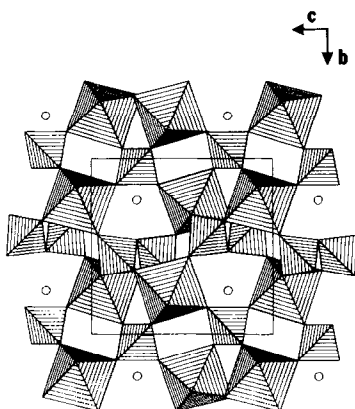


FIG. 2. A polyhedron representation of a layer in $\text{Cs}_2\text{Mo}_4\text{P}_6\text{O}_{12}$.

this method is +5.15, which is close to that based on the stoichiometry. The PO_4 tetrahedra, which share their corners with four MoO_6 octahedra, are quite regular, as shown by the O–O distances ranging from 2.460 to 2.520 Å. The P1–O distances

TABLE V
SELECTED INTERATOMIC DISTANCES (Å)
IN $\text{Cs}_4\text{Mo}_8\text{P}_{12}\text{O}_{52}$

Atom	Atom	Distance	Atom	Atom	Distance
Mo1	O2	1.68(2)	P1	O5	1.48(2)
Mo1	O4	1.96(2)	P1	O6	1.51(2)
Mo1	O1	2.01(2)	P1	O8	1.53(2)
Mo1	O26	2.02(2)	P1	O7	1.57(2)
Mo1	O3	2.03(2)	P2	O21	1.48(2)
Mo1	O5	2.25(2)	P2	O11	1.48(2)
Mo2	O10	1.68(2)	P2	O14	1.52(2)
Mo2	O9	1.96(2)	P2	O13	1.53(2)
Mo2	O13	2.00(2)	P3	O15	1.49(2)
Mo2	O8	2.06(2)	P3	O12	1.49(2)
Mo2	O11	2.07(2)	P3	O16	1.53(2)
Mo2	O12	2.19(2)	P3	O17	1.59(2)
Mo3	O18	1.62(2)	P4	O1	1.50(2)
Mo3	O14	1.99(2)	P4	O19	1.51(2)
Mo3	O16	2.00(2)	P4	O20	1.52(2)
Mo3	O6	2.05(2)	P4	O17	1.65(2)
Mo3	O15	2.08(2)	P5	O4	1.52(2)
Mo3	O19	2.16(2)	P5	O25	1.55(2)
Mo4	O22	1.65(2)	P5	O23	1.56(2)
Mo4	O25	1.96(2)	P5	O9	1.58(2)
Mo4	O23	2.00(2)	P6	O3	1.51(2)
Mo4	O20	2.02(2)	P6	O24	1.52(2)
Mo4	O21	2.08(2)	P6	O26	1.53(2)
Mo4	O24	2.17(2)	P6	O7	1.61(2)

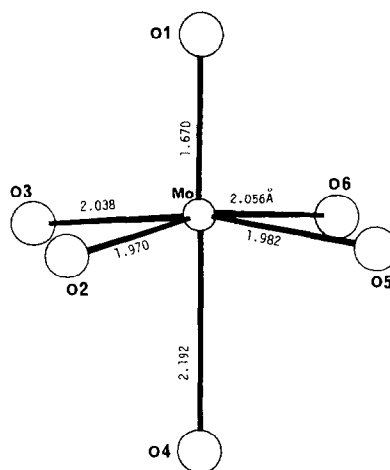


FIG. 3. The coordination of oxygen atoms around the molybdenum atom in $\text{Cs}_2\text{Mo}_4\text{P}_6\text{O}_{26}$.

(1.516–1.534 Å) and O–P1–O angles (107.5–112.5°) indicate that P1 is essentially located at the center of the tetrahedron. The pyrophosphate groups P_2O_7 share their corners with four MoO_6 octahedra. Each P_2O_7 group shares two oxygen atoms with the same MoO_6 octahedron. The two PO_4 tetrahedra forming the P_2O_7 group are also nearly regular ($d(\text{O}–\text{O}) = 2.462$ to 2.522 Å). However, the P2–O distances (1.492 to 1.602 Å) and O–P2–O angles (105.8–114.0°) indicate that the P2 atom is displaced from the center of its tetrahedron. Both the P2–O7–P2 angle (119.9°) and the configuration of the P_2O_7 group (Fig. 4) are rather similar to those observed in $\alpha\text{-K}_4\text{Mo}_8\text{P}_{12}\text{O}_{52}$. Nevertheless, both the PO_4 and P_2O_7 groups in $\text{Cs}_2\text{Mo}_4\text{P}_6\text{O}_{26}$ are slightly more distorted in comparison with the potassium compound.

On the basis of the above discussions, $\text{Cs}_2\text{Mo}_4\text{P}_6\text{O}_{26}$ can be formulated as $\text{Cs}_2(\text{MoO})_4(\text{PO}_4)_2(\text{P}_2\text{O}_7)_2$. It should be noted that the frameworks of the compounds $\text{Cs}_2\text{Mo}_4\text{P}_6\text{O}_{26}$ and $\alpha\text{-K}_4\text{Mo}_8\text{P}_{12}\text{O}_{52}$ are composed of the same building units, i.e., MoO molybdenyl groups, PO_4 tetrahedra, and pyrophosphate groups P_2O_7 . The structure

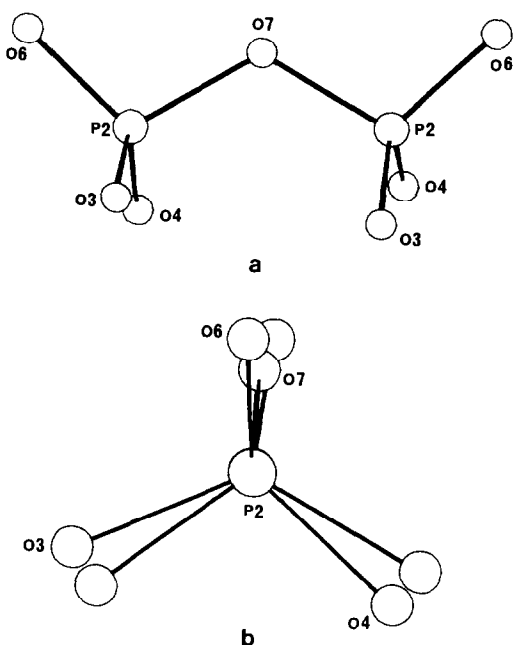


FIG. 4. A P_2O_7 group in $Cs_2Mo_4P_6O_{26}$. (a) View perpendicular to the $P \dots P$ vector and (b) view parallel to the $P \dots P$ vector.

types of these two molybdenyl phosphates are determined by the arrangements of the building units in the lattice, which in turn appear to be directed by the nature of the

counterions. The tunnels in the compound $\alpha\text{-K}_4\text{Mo}_8\text{P}_{12}\text{O}_{52}$ appear to be a little too small to accommodate the large Cs^+ ions because the calculated $Cs-O$ distance (3.03 Å) based on Cs^+ (1.67 Å, C.N. = 6) and O^{2-} (1.36 Å, C.N. = 3) (7) is larger than the observed $K-O$ distances (2.698 to 2.995 Å). Therefore, the $\alpha\text{-K}_4\text{Mo}_8\text{P}_{12}\text{O}_{52}$ structure has to be modified in order to accommodate the larger cations. As depicted in Fig. 5, a layer structure such as $Cs_2Mo_4P_6O_{26}$ can be generated from $\alpha\text{-K}_4\text{Mo}_8\text{P}_{12}\text{O}_{52}$ by displacing the neighboring building blocks by the specified distance. In $Cs_2Mo_4P_6O_{26}$ and Cs^+ is surrounded by six oxygen atoms at distances ranging from 3.256 to 3.300 Å in a geometry of trigonal antiprism. The Cs atom shows a large thermal parameter indicative of a positional disorder.

$Cs_4Mo_8P_{12}O_{52}$

This complicated structure presents an alternative modification of the $\alpha\text{-K}_4\text{Mo}_8\text{P}_{12}\text{O}_{52}$ structure to accommodate the large Cs^+ ions (Fig. 6). It consists of three different tunnels of which two are occupied by Cs^+ . In contrast to $Cs1$, which is in the center of the medium tunnel, $Cs2$ is located near the wall of the large tunnel. The large tunnels

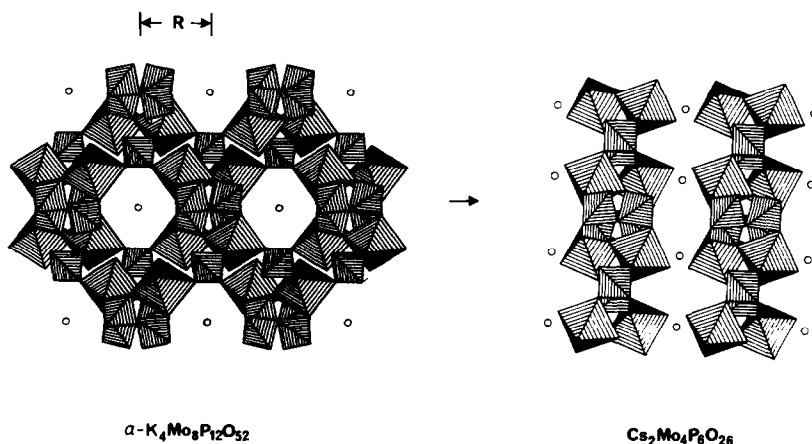


FIG. 5. $\alpha\text{-K}_4\text{Mo}_8\text{P}_{12}\text{O}_{52}$ – $Cs_2Mo_4P_6O_{26}$ transformation. A layer structure is generated from $\alpha\text{-K}_4\text{Mo}_8\text{P}_{12}\text{O}_{52}$ by displacing the neighboring building blocks by R .

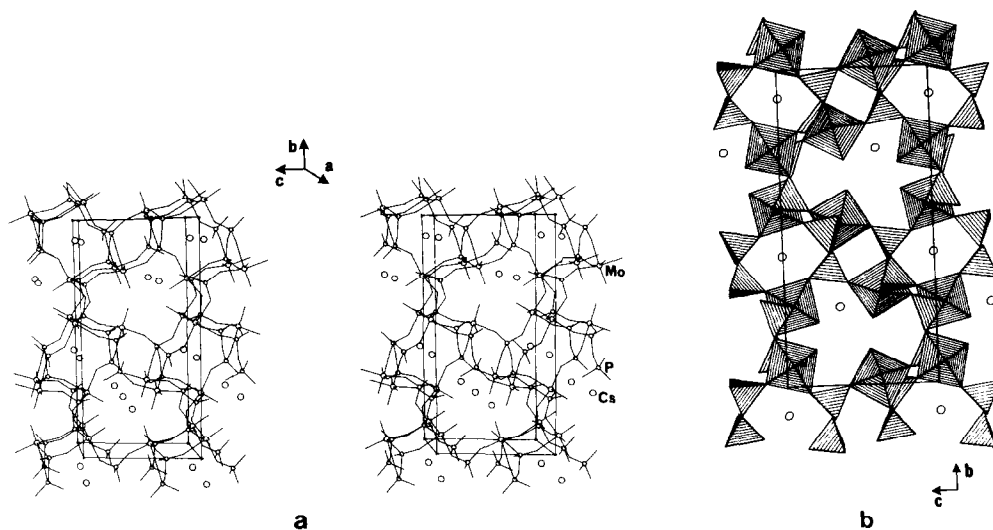


FIG. 6. (a) A stereoscopic view of the $\text{Cs}_4\text{Mo}_8\text{P}_{12}\text{O}_{52}$ structure. For clarity, the radii for oxygen atoms are set equal to zero. (b) A polyhedron representation of the $\text{Cs}_4\text{Mo}_8\text{P}_{12}\text{O}_{52}$ structure.

have empty sites available for more Cs^+ , suggesting the possibility of synthesizing a more reduced phase with higher content of the counter cation. Cs1 and Cs2 are surrounded by 12 and 10 oxygen atoms at distances ranging from 3.05 to 3.66 Å and 2.96 to 3.64 Å, respectively (Fig. 7). In comparison with the cesium atom in $\text{Cs}_2\text{Mo}_4\text{P}_6\text{O}_{26}$, those in $\text{Cs}_4\text{Mo}_8\text{P}_{12}\text{O}_{52}$ have considerably smaller thermal parameters indicative of stronger Cs–O bonds.

Interestingly, the framework of $\text{Cs}_4\text{Mo}_8\text{P}_{12}\text{O}_{52}$ is composed of the same building units as in $\alpha\text{-K}_4\text{Mo}_8\text{P}_{12}\text{O}_{52}$, i.e., eight MoO molybdenyl groups, four PO_4 tetrahedra, and four P_2O_7 groups. The coordination of each molybdenum atom is similar to that in $\text{Cs}_2\text{Mo}_4\text{P}_6\text{O}_{26}$, i.e., one very short and one very long Mo–O bond distance. Mo1 and Mo3 each shares its five corners with three P_2O_7 groups and one PO_4 tetrahedron. One of the pyrophosphate groups shares two oxygen atoms with the molybdenum atom. Mo2 and Mo4 each shares its five oxygen atoms with three PO_4 tetrahedra and two pyrophosphate groups. Using the bond–

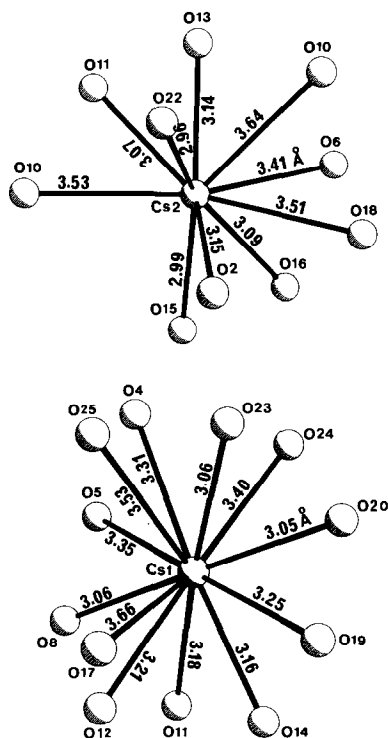


FIG. 7. The coordination of oxygen atoms around Cs1 and Cs2 in $\text{Cs}_4\text{Mo}_8\text{P}_{12}\text{O}_{52}$. The e.s.d. for each Cs–O bond distance is 0.02 Å.

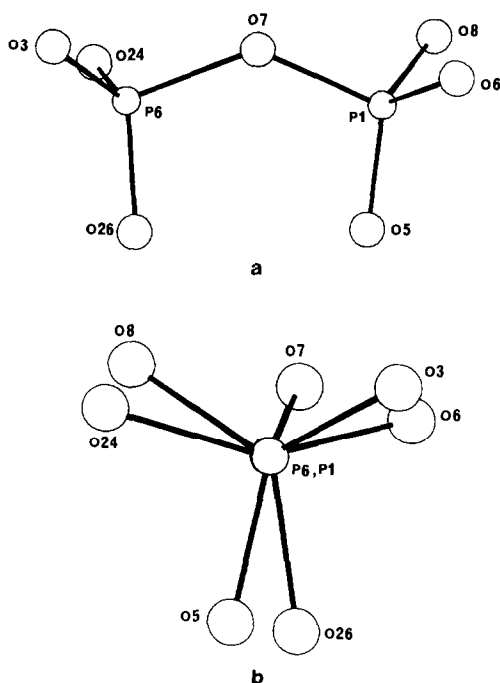


FIG. 8. A pyrophosphate group in $\text{Cs}_4\text{Mo}_8\text{P}_{12}\text{O}_{52}$. (a) View perpendicular to the P . . . P vector and (b) view parallel to the P . . . P vector.

length bond–strength relationship discussed above for the Mo–O bond, we have found that the effective charges on the four molybdenum atoms are +5.1, +5.0, +5.4, and +5.3 for Mo1, Mo2, Mo3, and Mo4, respectively. The phosphate groups, P(2)O₄ and P(5)O₄, each share its four corners with four MoO₆ octahedra. The pyrophosphate groups, P(1)P(6)O₇ and P(3)P(4)O₇, are similar in configuration and each shares its six corners with five MoO₆ octahedra. Each pyrophosphate group shares two oxygen atoms with one of the five octahedra. Both the configurations and the P–O–P bond angles (P1–O7–P6 = 131°, P3–O17–P4 = 129°) of the pyrophosphate groups in $\text{Cs}_4\text{Mo}_8\text{P}_{12}\text{O}_{52}$ are rather different from those in the layer structure (Fig. 8). On average, the different polyhedra in $\text{Cs}_4\text{Mo}_8\text{P}_{12}\text{O}_{52}$ are slightly more distorted than those in $\text{Cs}_2\text{Mo}_4\text{P}_6\text{O}_{26}$ on the basis of

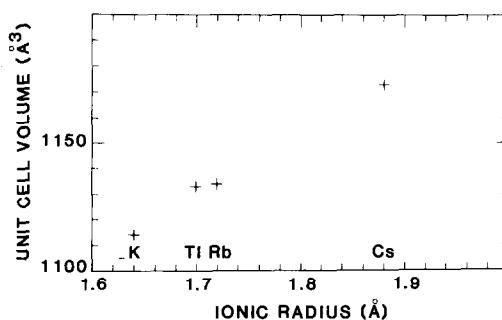


FIG. 9. Cell volume vs the ionic radius of the counter cation for some compounds with the $\text{Cs}_4\text{Mo}_8\text{P}_{12}\text{O}_{52}$ structure.

the oxygen–oxygen distances. However, it should be noted that the e.s.d.'s for bond distances in $\text{Cs}_4\text{Mo}_8\text{P}_{12}\text{O}_{52}$ are considerably higher.

A plot (Fig. 9) of the unit cell volume of $\text{M}_4\text{Mo}_8\text{P}_{12}\text{O}_{52}$ vs the ionic radii (C.N. = 12) (7) of the counter cations shows that the “ $\text{Mo}_8\text{P}_{12}\text{O}_{52}$ ” framework is flexible. An attempt to synthesize isostructural compounds containing counter cations smaller than K^+ has revealed that more new structures exist in this system. A variety of frameworks which are built up from corner-sharing MoO₆ octahedra and PO₄ tetrahedra have been observed. Further research on these materials is in progress.

References

1. A. LECLAIRE, J. C. MONIER, AND B. RAVEAU, *J. Solid State Chem.* **48**, 147 (1983).
2. A. LECLAIRE, J. C. MONIER, AND B. RAVEAU, *J. Solid State Chem.* **59**, 301 (1985).
3. D. T. CROMER AND J. T. WABER, “International Tables for X-Ray Crystallography,” Vol. IV, Table 2.2A, Kynoch Press, Birmingham, England (1974).
4. J. A. IBERS AND W. C. HAMILTON, *Acta Crystallogr.* **17**, 781 (1964).
5. D. T. CROMER, “International Tables for X-Ray Crystallography,” Vol. IV, Table 2.3.1, Kynoch Press, Birmingham, England (1974).
6. I. D. BROWN AND K. K. WU, *Acta Crystallogr., Sect. B* **32**, 1957 (1976).
7. R. D. SHANNON, *Acta Crystallogr., Sect. A* **32**, 751 (1976).